Relativistic mean-field model with density-dependent meson-nucleon couplings

Kenta Minagawa, Masahiro Kawabata and Koichi Saito

Department of Physics, Faculty of Science and Technology, Tokyo University of Science, Noda 278-8510, Japan

Within the relativistic mean-field approach, we extend the Miyazaki model, where the NNσ and NNω interactions are modified to suppress the couplings between positive- and negative-energy states of a nucleon in matter. Assuming appropriate density-dependence of the meson-nucleon couplings, we study nuclear matter and finite nuclei. The model can reproduce the observed properties of ^{16}O and ^{40}Ca well. We also examine if the model is *natural*.

Recently, the relativistic mean-field approach with density-dependent meson-nucleon couplings draws much attention.[1)] It is an effective model for the Dirac-Brueckner-Hartree-Fock (DBHF) theory,[2)] which can reproduce the saturation property of nuclear matter using the one-boson exchange potentials extracted from the nucleon-nucleon scattering data. In the DBHF calculation, the relativistic effect provides a strong density-dependent repulsion, which is originated from the nucleon-antinucleon pair term (Z graph), and it is vital to obtain the nuclear saturation property. It should be noticed that a nuclear model based on the quark substructure of a nucleon, for example, the quark-meson coupling (QMC) model,[3)] the quark-mean field (QMF) model,[4)] also gives density-dependent meson-nucleon couplings through the scalar field in a nuclear medium, namely the scalar polarizability.[3)] Thus, it seems quite natural that the meson-nucleon couplings depend on the nuclear environment.

About a decade ago, Miyazaki[5)] has proposed an interesting, relativistic mean-field model for nuclear matter, in which the NNσ and NNω vertices are modified to reduce the couplings between positive- and negative-energy states of the in-medium nucleon (the $+-$ couplings). Although the $+-$ couplings play an important role in the relativistic nuclear models including nucleon-nucleus (NA) scattering (with the relativistic impulse approximation (RIA)) at intermediate energies, it is known that the effect of the coupling to negative states is too strong to produce the NA scattering observables at low energies.[6)] Tjon and Wallace have remedied this problem by developing a generalized RIA, in which the different $+-$ couplings from the usual RIA are introduced.[6)] The vertex modification studied by Miyazaki[5)] may enable us to include such variation of the $+-$ couplings at the relativistic mean-field level. The modified vertices finally result in the density-dependent NNσ and NNω couplings, which can simultaneously reproduce the nuclear matter properties and the Dirac scalar and vector optical potentials given by the DBHF calculation.

In this Letter, we generalize the Miyazaki model, and study not only the nuclear matter properties but also single-particle energies of finite nuclei. Lastly, we discuss *naturalness* of the model.[7)]

We now modify the vertices of NNσ and NNω couplings using the energy projection operators, $\Lambda^{\pm}(p) = (\pm\not{p} + M)/2M$, where p is the four-momentum of a nucleon and M is the mass. Since the vertex, $\Gamma(= I \text{ or } \gamma^{\mu})$, is expressed by

$$\Gamma = \Lambda^{+}(p')\Gamma\Lambda^{+}(p) + \Lambda^{-}(p')\Gamma\Lambda^{-}(p) + \Lambda^{+}(p')\Gamma\Lambda^{-}(p) + \Lambda^{-}(p')\Gamma\Lambda^{+}(p), \quad (1)$$

it may be possible to vary the strength of the $+-$ couplings, introducing two parameters, $0 \le \lambda_1, \lambda_2 \le 1$, as[5]

$$\Gamma \to \lambda_1[\Lambda^{+}(p')\Gamma\Lambda^{+}(p) + \Lambda^{-}(p')\Gamma\Lambda^{-}(p)] + \lambda_2[\Lambda^{+}(p')\Gamma\Lambda^{-}(p) + \Lambda^{-}(p')\Gamma\Lambda^{+}(p)], \quad (2)$$

$$= \frac{(\lambda_1 - \lambda_2)\not{p}'\Gamma\not{p} + (\lambda_1 + \lambda_2)\Gamma M^2}{2M^2}. \quad (3)$$

In the original Miyazaki model,[5] λ_1 is chosen to be unity for the scalar (I) vertex, while λ_2 is unity for the vector (γ^{μ}) vertex, because the parameters are supposed to be constants. However, in general, the strength of the $+-$ couplings may depend on the nuclear environment through the Pauli blocking, Z graphs etc.[8] To take account of those effects in the model, we here suppose that λ simply depends on the nuclear density, ρ_v:

$$\lambda = 1 - a\left(\frac{\rho_v}{\rho_0}\right)^b, \quad (4)$$

where ρ_0 is the saturation density, and each λ has two parameters, a and b. Note that, in the limit $\rho_v \to 0$, Γ is identical to the original form Eq.(1).

Using the vertex (3) and the mean-field approximation for the meson fields, the Lagrangian density is given by[5]

$$\begin{aligned}\mathcal{L} &= \bar{\psi}(\not{p} - M)\psi - \frac{1}{2}m_\sigma^2\sigma^2 + \frac{1}{2}m_\omega^2\omega^2 \\ &+ \frac{g_\sigma}{2M^2}[(\lambda_1^s - \lambda_2^s)(\bar{\psi}\overleftarrow{\not{p}})(\not{p}\psi) + (\lambda_1^s + \lambda_2^s)M^2\bar{\psi}\psi]\sigma \\ &- \frac{g_\omega}{2M^2}[(\lambda_1^v - \lambda_2^v)(\bar{\psi}\overleftarrow{\not{p}})\gamma^0(\not{p}\psi) + (\lambda_1^v + \lambda_2^v)M^2\bar{\psi}\gamma^0\psi]\omega, \end{aligned} \quad (5)$$

where σ and ω are respectively the mean-field values of the σ and ω mesons, and $\lambda_i^{s(v)}$ $(i = 1, 2)$ is the parameter for the scalar (vector) vertex. The meson mass and the NN$\sigma(\omega)$ coupling constant in vacuum are respectively denoted by $m_{\sigma(\omega)}$ and $g_{\sigma(\omega)}$.

Following the prescription explained in Ref.[5], we can construct an *effective* Lagrangian density, in which the effect of variation of the $+-$ couplings in matter is included,

$$\mathcal{L}_{\text{eff}} = \bar{\psi}(\not{p} - \gamma^0 U_v - M^*)\psi - \frac{1}{2}m_\sigma^2\sigma^2 + \frac{1}{2}m_\omega^2\omega^2, \quad (6)$$

where the effective nucleon mass, M^*, and the Dirac scalar, U_s, and vector, U_v, potentials in matter are defined as

$$M - M^* = g_\sigma^*\sigma = -U_s, \qquad U_v = g_\omega^*\omega, \quad (7)$$

with the effective coupling constants

$$g_\sigma^* = \frac{1}{2}[(\lambda_1^s + \lambda_2^s) + (\lambda_1^s - \lambda_2^s)(m^{*2} - v^2)]g_\sigma, \tag{8}$$

$$g_\omega^* = \frac{1}{2}[(\lambda_1^v + \lambda_2^v) - (\lambda_1^v - \lambda_2^v)(m^{*2} - v^2)]g_\omega, \tag{9}$$

$m^* = M^*/M$ and $v = U_v/M$. Note that, when $\lambda_1^s = \lambda_2^v = 1$, the effective coupling constants coincide with those in the Miyazaki model.

The energy per nucleon, W, for symmetric nuclear matter is then written by

$$W = \frac{3}{4}E_F^* + \frac{1}{4}M^*\frac{\rho_s}{\rho_v} + U_v - M + \frac{2M}{C_s\hat{\rho}}\left[\frac{1-m^*}{\lambda_1^s + \lambda_2^s + (\lambda_1^s - \lambda_2^s)(m^{*2} - v^2)}\right]^2 - \frac{2M}{C_v\hat{\rho}}\left[\frac{v}{\lambda_1^v + \lambda_2^v - (\lambda_1^v - \lambda_2^v)(m^{*2} - v^2)}\right]^2, \tag{10}$$

where $E_F^* = (k_F^2 + M^{*2})^{1/2}$ (k_F the Fermi momentum), $\rho_v = 2k_F^3/3\pi^2$, $\hat{\rho} = \rho_v/\rho_0$, $C_{s(v)} = g_{\sigma(\omega)}^2\rho_0/m_{\sigma(\omega)}^2 M$, and $\rho_s = (M^*/\pi^2)[k_F E_F^* - M^{*2}\ln((k_F + E_F^*)/M^*)]$ (the scalar density).

From the self-consistency conditions, $(\partial W/\partial m^*) = 0$ and $(\partial W/\partial v) = 0$, which the meson fields should satisfy, one finds

$$C_s = \frac{4c}{a_s^3 b_s \hat{\rho}}(1 - m^*), \qquad C_v = \frac{4c}{a_v^3 b_v \hat{\rho}}v, \tag{11}$$

where

$$a_s = \lambda_1^s + \lambda_2^s + (\lambda_1^s - \lambda_2^s)(m^{*2} - v^2), \tag{12}$$

$$a_v = \lambda_1^v + \lambda_2^v - (\lambda_1^v - \lambda_2^v)(m^{*2} - v^2), \tag{13}$$

$$b_s = \left[\lambda_1^v + \lambda_2^v - (\lambda_1^v - \lambda_2^v)(m^{*2} + v^2)\right]\frac{\rho_s}{\rho_v} - 2(\lambda_1^v - \lambda_2^v)m^* v, \tag{14}$$

$$b_v = \lambda_1^s + \lambda_2^s - (\lambda_1^s - \lambda_2^s)(m^{*2} - 2m^* + v^2) + 2(\lambda_1^s - \lambda_2^s)(1 - m^*)v\frac{\rho_s}{\rho_v}, \tag{15}$$

$$c = [\lambda_1^s + \lambda_2^s - (\lambda_1^s - \lambda_2^s)(m^{*2} - 2m^* + v^2)][\lambda_1^v + \lambda_2^v - (\lambda_1^v - \lambda_2^v)(m^{*2} + v^2)] + 4(\lambda_1^s - \lambda_2^s)(\lambda_1^v - \lambda_2^v)(1 - m^*)m^* v^2. \tag{16}$$

Giving the λ parameters, the coupling constants in vacuum, g_σ and g_ω, are determined so as to fulfill the saturation condition, $\partial W/\partial\hat{\rho}|_{\hat{\rho}=1} = 0$ and $W(\hat{\rho} = 1) = -15.75$MeV ($\rho_0 = 0.15$ fm^{-3}). Using those coupling constants, one can calculate the effective nucleon mass (m^*) and the vector potential (v) at any density.

In the present calculation, we, however, set that $\lambda_1^s = \lambda_2^v = 1 - a_A(\rho_v/\rho_0)^{b_A}$ and $\lambda_2^s = \lambda_1^v = 1 - c_A(\rho_v/\rho_0)^{d_A}$ to reduce the total number of parameters. (We call this "type A".) Thus, for type A the density-dependence of the NNσ coupling is identical to that of the NNω coupling, i.e., $g_\sigma^*/g_\sigma = g_\omega^*/g_\omega$ (see Eqs.(8) and (9)). This choice may be justified, because it has already been found in Ref.[5] that the case of $\lambda_1^s = \lambda_2^v$ and $\lambda_2^s = \lambda_1^v$ gives the best result for the nuclear matter properties. In contrast, we shall also study an alternative: $\lambda_1^s = \lambda_1^v = 1 - a_B(\rho_v/\rho_0)^{b_B}$ and $\lambda_2^s = \lambda_2^v = 1 - c_B(\rho_v/\rho_0)^{d_B}$. (We call this "type B".) Thus, each type eventually has four parameters ($a \sim d$) to fit the observed data.

Table I. Parameter sets for type A and B. The nuclear incompressibility K (in MeV) is also shown.

type	a	b	c	d	K
A	0.15	0.9	0.26	0.1	239.3
B	0.40	0.3	0.37	0.3	202.9

Now we are in a position to show our numerical results. We determine the coupling constants, g_σ and g_ω, so as to exactly reproduce the saturation condition of nuclear matter. In addition, the parameters, $a \sim d$, are tuned so as to produce the scalar U_s and vector U_v potentials of the DBHF calculation and the observed incompressibility ($K = 210 \pm 30$ MeV) as precisely as possible.

We find that $g_\sigma = 12.24(16.97)$ and $g_\omega = 14.97(20.69)$ for type A (B). In Table I, we list the parameter sets for type A and B. In Figs. 1 and 2, the scalar and vector

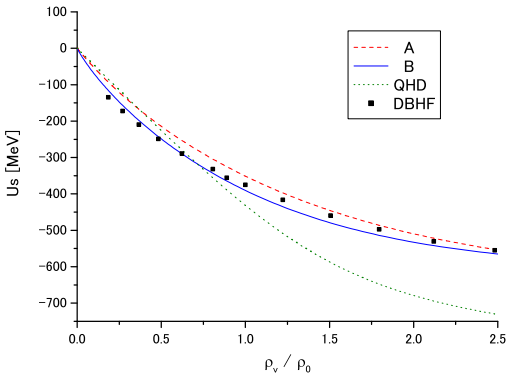

Fig. 1. The scalar potential. The dashed, solid and dotted curves are, respectively, for type A, B and QHD. The DBHF result is shown by solid squares.

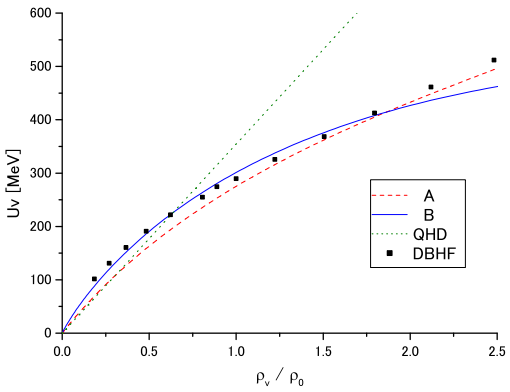

Fig. 2. The vector potential. The curves are labeled as in Fig. 1.

potentials calculated with the present parameter sets are shown, together with the results of DBHF calculation[2] and Quantum Hadrodynamics (QHD).[9] The DBHF result is well reproduced by the present model up to $\rho_v/\rho_0 = 2.0 \sim 2.5$. We again see from Table I that $g^*_\sigma/g_\sigma \simeq g^*_\omega/g_\omega$ even in type B because $b_B = d_B$ and $a_B \approx c_B$. Thus, for fitting the scalar and vector potentials of the DBHF calculation and the observed incompressibility simultaneously, it may be favorable that the density-dependence of the NNσ interaction is very close to that of the NNω interaction.

Table II. Binding energy per nucleon W (in MeV), rms charge radius r_{ch} (in fm) and difference between nuclear radii for neutrons and protons $r_n - r_p$ (in fm). The QHD result is also included.

		^{40}Ca			^{16}O		
	m_σ(MeV)	$r_{\rm ch}$	W	$r_n - r_p$	$r_{\rm ch}$	W	$r_n - r_p$
A	463.4	3.482	5.78	-0.080	2.83	4.22	-0.047
B	513.0	3.482	7.33	-0.074	2.77	6.06	-0.041
QHD	523.8	3.482	6.24	-0.055	2.75	4.85	-0.033
Exp.		3.482	8.45	0.05±0.05	2.73	7.98	0

Table III. Model predictions for the energy spectrum of ^{40}Ca.

	Proton				Neutron			
	A	B	QHD	Exp.	A	B	QHD	Exp.
$1s_{1/2}$	45.8	48.5	46.7	50±10	55.1	57.6	55.0	51.9
$1p_{3/2}$	30.2	32.9	30.8	34±6	38.7	41.3	38.7	36.6
$1p_{1/2}$	26.7	29.2	25.3	34±6	35.2	37.7	33.2	34.5
$1d_{5/2}$	15.6	17.9	15.2	15.5	23.3	25.6	22.6	21.6
$2s_{1/2}$	11.5	12.6	7.2	10.9	19.2	20.4	14.4	18.9
$1d_{3/2}$	10.2	11.9	6.7	8.3	17.9	19.6	14.1	18.4

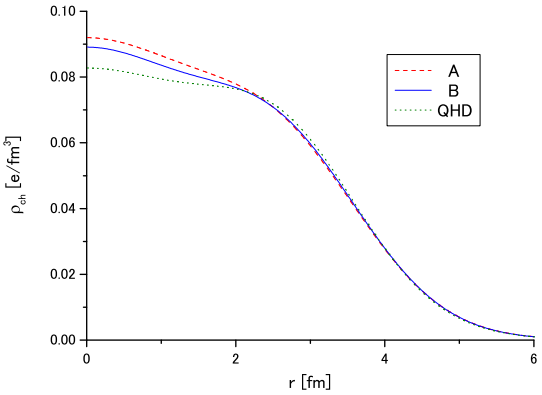

Fig. 3. Charge density distribution for ^{40}Ca compared with that of QHD. The curves are labeled as in Fig. 1.

For finite nuclei, Eq.(6) gives a set of coupled non-linear differential equations, which may be solved by a standard iteration procedure.[10] For example, we have calculated the properties of ^{16}O and ^{40}Ca, and the result is presented in Table II. In the calculation, we have adjusted the σ mass (m_σ) so as to yield the observed root-mean-square (rms) charge radius of ^{40}Ca: $r_{ch}(^{40}\mathrm{Ca}) = 3.48$ fm. In Table III, we give the single-particle energies for ^{40}Ca. We can see from the table that the model, especially type B, produces the good result. The spin-orbit force in the present model is thus sufficient to reproduce the observed energy levels and it is comparable to that of QHD. The charge density distribution for ^{40}Ca is also illustrated in Fig. 3, together with the QHD result. Note that the observed distribution, which is not shown here, is very close to that of type B.

Finally, we shall examine the present model using Georgi's "naive dimensional analysis" (NDA).[7),11)] In general, an effective field theory at low energy will contain an infinite number of interaction terms, which incorporate the compositeness of the low-energy degrees of freedom, i.e., hadrons, and it is then expected to involve numerous couplings which may be nonrenormalizable. The NDA gives a systematic way to manage such complicated, effective field theories. After extracting the dimensional factors and some appropriate counting factors using NDA, the remaining *dimensionless* coefficients are all assumed to be of order *unity*. This is the so-called *naturalness assumption*. If theory is *natural*, one can then control the effective Lagrangian, at least at the tree level. In the present case, the model involves the NNσ and NNω interactions. Using NDA, we then find that the dimensionless coefficients corresponding to those couplings are all smaller than 2.0. Thus, the model is *natural*.

In summary, we have extended the Miyazaki model,[5)] where the NNσ and NNω

couplings are modified to suppress the $+-$ couplings, and studied two (A and B) types of density-dependent meson-nucleon vertices. Assuming an appropriate density form at the vertex, the parameters are adjusted so as to produce the scalar and vector potentials of the DBHF calculation and the observed incompressibility K as precisely as possible. The density-dependence such as $g_\sigma^*/g_\sigma \approx g_\omega^*/g_\omega$ may be eventually favorable for fitting the DBHF result and the observed nuclear data. Using such coupling constants, we have studied the properties of nuclear matter and finite nuclei (^{16}O and ^{40}Ca). The model can reproduce the experimental data well. Furthermore, NDA tells us that the model is *natural*. It is thus vital to include appropriate density-dependence of the meson-nucleon interactions in the relativistic mean-field approach, which may be attributed to many-body effects (like the Pauli exclusion) and the quark substructure of an in-medium nucleon.[3)]

References

1) R. Brockmann and H. Toki, Phys. Rev. Lett. **68** (1992), 3408; C. Fuchs, H. Lenske and H.H. Wolter, Phys. Rev. C **52** (1995), 3043; H. Shen, Y. Sugahara and H. Toki, Phys. Rev. C **55** (1997), 1211.
2) R. Brochmann and R. Machleidt, Phys. Rev. C **42** (1990), 1965; G.Q. Li, R. Machleidt and R. Brockmann, Phys. Rev. C **45** (1992), 2782.
3) K. Saito, K. Tsushima and A.W. Thomas, Prog. Part. Nucl. Phys. **58** (2007), 1; P.A.M. Guichon, Phys. Lett. B **200** (1988), 235; K. Saito and A.W. Thomas, Phys. Lett. B **327** (1994), 9.
4) H. Toki, U. Meyer, A. Faessler and R. Brochmann, Phys. Rev. C **58** (1998), 3749; H. Shen and H. Toki, Phys. Rev. C **61** (2000), 045205.
5) K. Miyazaki, Prog. Theor. Phys. **93** (1995), 137.
6) J.A. Tjon and S.J. Wallace, Phys. Rev. C **32** (1985), 267; ibid. **32** (1985), 1667.
7) A. Manohar and H. Georgi, Nucl. Phys. B **234** (1984), 189; H. Georgi, Phys. Lett. B **298** (1993), 187.
8) M.R. Anastasio, L.S. Celenza, W.S. Pong and C.M. Shakin, Phys. Rep. **100** (1983), 327.
9) B.D. Serot and J.D. Walecka, Adv. Nucl. Phys. **16** (1986), 1.
10) K. Saito, K. Tsushima and A.W. Thomas, Nucl. Phys. A **609** (1996), 339.
11) K. Saito, K. Tsushima and A.W. Thomas, Phys. Lett. B **406** (1997), 287.